IRIS reactor core with thorium fuel

Alrwashdeh MOHAMMAD* YU Ganglin WANG Kan

Department of Engineering physics, Tsinghua University, Beijing 100084, China

Abstract This work is aimed at running the first IRIS reactor core with mixed thorium dioxide fuel (ThO_2-UO_2 and ThO_2-PuO_2). Calculations are performed by using Dragon 4.0.4 and Citation codes. The results show the multiplication factor (K_{eff}) for central and peripheral assemblies as a function of burnup. To ensure the proliferation resistance, the value of ^{235}U enrichment is ≤ 20%. The K_{eff} is calculated using Dragon 4.0.4 for a single fuel rod and the model developed to fuel assembly, while the whole core was calculated using Citation code. For a fuel burnup, the use of increased enrichment fuel in the IRIS core leads to high reserve of reactivity, which is compensated with an integral fuel burnable absorber. The self-shielding of boron is in an IRIS reactor fuel. The effect of increased enrichment to the burn-up rates, and burnable poison distribution on the reactor performance, are evaluated. The equipment used in traditional light water reactors is evaluated for designing a small unit IRIS reactor.

Key words Long life reactor, High burnup, Burnable absorber

1 Introduction

International Reactor Innovative and Secure (IRIS) is an advanced small –to- medium- size (1 GWt) PWR with primary system[1-3]. The innovative design and core physics analysis was performed by Westinghouse Company for both Uo_2 fuel and MOX fuel. The interesting use of thorium as a fuel in light water reactors was due to long refueling interval and high burn-up of thorium fuel. ThO_2-UO_2 core designed can have a longer cycle, which is required less enrichment and less high-level waste, than UO_2 core.

To design a smart long life nuclear power plant, with high burn-up fuel and proliferation resistance, the fuel assemblies should have high concentration of the fissile materials like ^{235}U and ^{239}Pu. Some studies[4,5] show that the thorium based fuel performed better than uranium based fuel, where 70% plutonium are consumed during the cycle. And the burn-up achieved by Th-based reactor is 1.4 to 4.6 folds higher than the U-based reactor. Th-based reactor has an extra advantage which reducing the amount of the long life nuclides.

Basics researches on thorium fuel cycle have been conducted in the United States of America, Russia, Germany, India, United Kingdom, and Japan[6]. The THRT reactor developed by Germany which is 300 MWe reactor with thorium/high enriched Uranium fuel[7]. The Fort, St. reactor developed by United states using thorium/high enriched Uranium fuel, and it used graphite as moderator and helium to cooled the reactor[8].

In order to meet the global energy requirements, achieve safety and efficiency level, and address proliferation issue, different kinds of innovative reactors will be needed. The design of a small light water reactor core demands a comprehensive understanding of the physics, adequate and efficient computer system, and design methodology.

The use of thorium in light water reactors have been inspired in the recent years, due to concerns accompanied with the limited uranium fuel resources and the perceived non-proliferation advantages of the utilization of thorium in the fuel cycle.

Supported by 973 Program（2007CB209807）

* Corresponding author. *E-mail address:* rawashdeh.80@gmail.com

Received date: 2011-03-24

2 Core neutronic design

2.1 Core parameters

The parameters in Table 1 were designed for the IRIS reactor cores. Using the same fuel parameters as the Westinghouse Robust fuel 17×17, but some changes in lattice pitch and plenum volume were made. The number densities are shown in Table 2.

Table 1 Iris reactor core parameters

Parameters	Values
Fuel assembly total length / m	5.207 [2]
Fuel inventory / tU	48.5 [2]
Average core power density/ kW·L^{-1}	51.26[2]
Specific power* / kW·kg^{-1}-HM	20.6186[2]
Fuel materials	ThO_2,75; UO_2, 25 ThO_2,75; PuO_2, 25
U enrichment / %	^{235}U,19.5; ^{238}Pu,2.5 ^{239}Pu,54.1; ^{240}Pu, 23.9 ^{241}Pu,12.7; ^{242}Pu, 6.9
Rod array	Square, 17×17 XL[2]
Number of fuel assemblies	89[2]
Number of fuel rods/assembly	264[2]
Fuel pellet diameter / mm	8.19[2]
Pellet-clad gap / mm	0.082[10]
Clad thickness / mm	0.572[10]
Outer diameter of fuel rods / mm	9.5[2, 10]
Pitch (center-to-center) / mm	12.54[10]
P/D	1.32[10]
Active core height (core barrel) /cm	426.7[10]

* specific power = core thermal power/fuel inventory

2.2 Fuel number densities

From the Tables 1 and 2, the fuel number densities for both mixed ThO_2-UO_2 fuel and mixed ThO_2-PuO_2 fuel, were the theoretical density consisting of 7 % Th, 25% U with enrichment up to 19.5% ^{235}U, and the theoretical density consisting of 75% Th, 25% Pu isotopes with enrichment up to 2.5% ^{238}Pu, 54.1% ^{239}Pu, 23.9% ^{240}Pu, 12.7% ^{241}Pu and 6.9% ^{242}Pu.

Table 2 ThO_2-UO_2 fuel number densities

Materials	Isotopes	Number density /atom·barn^{-1}·cm^{-1}
Fuel pellet:	^{232}Th	0.0161665
	^{235}U	0.0011401
ThO_2±UO_2	^{238}U	0.0046471
	^{16}O	0.0439075
	Zr	0.0425391
	^{118}Sn	1.20902×10^{-4}
	Fe	8.84265×10^{-5}
Clad: Zircalloy	Cr	7.59779×10^{-5}
(Zirc$_2$)	^{14}N	1.41059×10^{-4}
	H	0.0430769
Coolant: water	^{16}O	0.0215384
Fuel pellet:	^{238}Pu	0.1523842
ThO_2±PuO_2	^{239}Pu	0.0032742
	^{240}Pu	0.0014403
	^{241}Pu	7.620058×10^{-4}
	^{242}Pu	4.120032×10^{-4}
Clad: Zircalloy	Zr	0.0425391
(Zirc$_2$)	^{118}Sn	1.20902×10^{-4}
	Fe	8.84265×10^{-5}
	Cr	7.59779×10^{-5}
	^{14}N	1.41059×10^{-4}
	H	0.043077
Coolant: water	^{16}O	0.021538

3 Methods

3.1 Dragon 4.0.4

Dragon 4.0.4, and the WIMSD4 library, were used to calculate the burn-up for a typical pin cell model representing unit cell lattice of Westinghouse PWR. Fig.1 shows that the multiplication factor (K_{eff}) and reactivity decrease with increasing burn-up for a single pin, until the end of the cycle.

In Fig.2a the K_{eff} and reactivity decrease with increasing burn-up for a standard fuel assembly of the IRIS reactor with ThO_2-UO_2 fuel peripheral assembly. The reactivity, defined as $p=(k-1)/k$, where p is sum of the positive and negative reactivity of the fissile material. The negative reactivity is caused by fission products that absorb neutrons and act as neutron poisons, such as xenon and samarium.

The first drop in the curves is due to the start operation with fresh fuel, and the negative component of the reactivity is due to the build up of the actinide fission products. The positive reactivity of the fuel decreases almost linearly with the increasing fuel burn-up.

The cycle is ended with accumulated fission fragment and their decay products, particularly ^{135}Xe. They have large absorption cross-sections for thermal neutron. And the K_{eff} value has an inverse proportional to their densities, due to the changed reactor reactivity in the core. In Fig.2b, the K_{eff} and reactivity decrease with increasing burn-up the peripheral assembly with enrichment 14% ^{235}U and 45% ^{239}Pu.

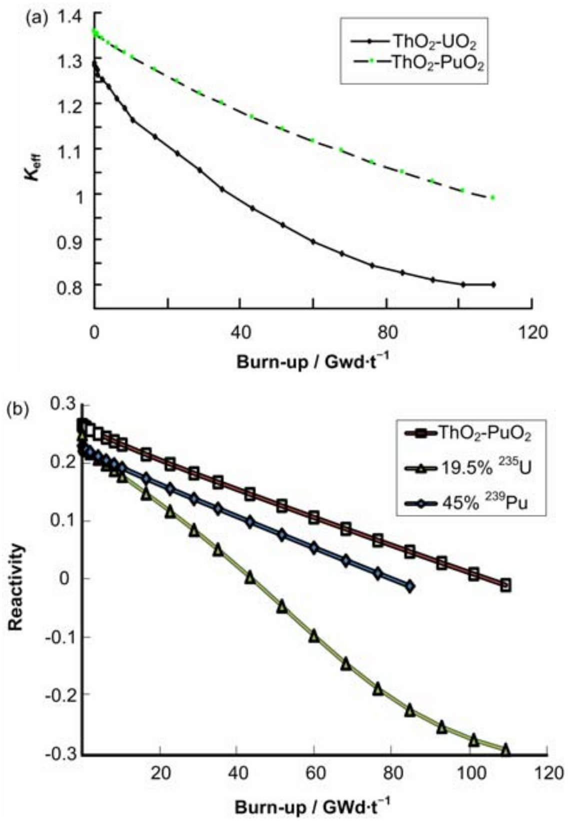

Fig.1 K_{eff} and reactivity *vs.* burn-up for single ThO_2-UO_2 pin.

The neutron leakage decreases with increasing amount of moderator in the core (i.e. the moderator-to-fuel ratio N_m/N_u increases). Increased neutron absorption in the moderator causes a decrease in the thermal utilization factor, but insufficient moderator in the core (N_m/N_u decreases) causes longer slowing down time and results in a greater loss of neutrons by resonance absorption.

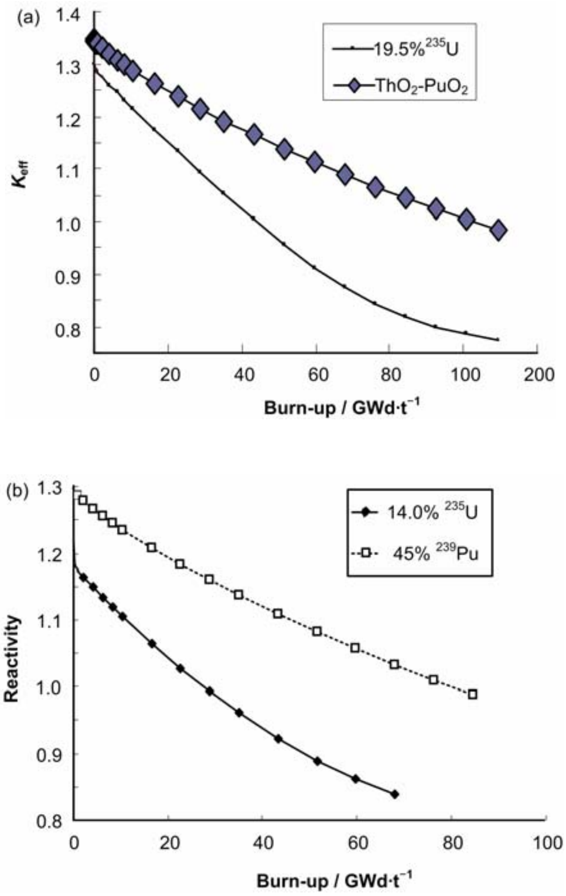

Fig.2 K_{eff} and reactivity *vs.* burn-up for ThO_2-UO_2 fuel peripheral assemblies.

3.2 Fuel assembly with IFBA

Calculations were done for IRIS reactor assembly with adding integral fuel burnable absorber (IFBA) at different concentrations. This was performed based on Dragon 4.0.4 calculation. Fig.3a shows the K_{eff} as a function of burn-up for ThO_2-UO_2 fuel, with the IFBA concentration of 0.45 to 0.933.

At the beginning, the K_{eff} decreases due to the ^{10}B, which has a high neutron absorption cross section. After a certain period of time, the values of K_{eff} begins to increase because the ^{10}B becomes other isotopes by absorption of the neutrons. And as the burn-up increases, the distance decreases gradually among the curves, which meet at about 30000 MWd·t^{-1} and higher burn-up values. Fig.3b shows the K_{eff} *vs.* burn-up for ThO_2-PuO_2 fuel at 0.561 IFBA.

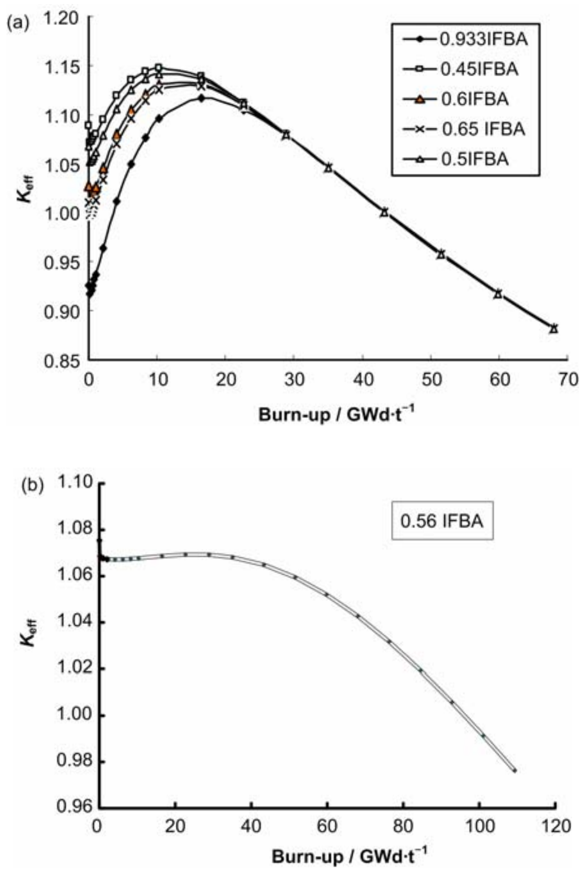

Fig.3 Fuel assembly with different IFBA concentration for ThO_2-UO_2 fuel (a) and ThO_2-PuO_2 fuel (b).

3.3 Citation-LDI2

Citation codes were used to perform the core calculations. It has been used at ORNL on a production basis for solving problems involving the finite- difference diffusion-theory representing of neutron transport theory. The ThO_2-UO_2 fuel is enriched ^{235}U (19.5%), but the enrichment is 14.0% in the core periphery and the blankets, while the ThO_2-PuO_2 fuel is enriched ^{239}Pu (54.1%) and 45% enrichment in the core periphery and the blankets. Fig.4 shows the IRIS core configuration. Fig.5 shows the IFBA distribution for ThO_2-UO_2 and ThO_2-PuO_2 cores. In Fig.6 the $K_{\rm eff}$ decreases with increasing core burn-up for both ThO_2-UO_2 and ThO_2-PuO_2 cores.

The infinite multiplication factor $K_{\rm eff}$ is plotted as a function of burn-up, for a maximum of 80 GWd/t. There is a sharp decrease in $K_{\rm eff}$ as ^{135}Xe and ^{149}Sm build up in the fresh fuel. The criticality in the annular fuel is higher due to the higher water-to-metal ratio and a Doppler coefficient effect contribution because of lower average fuel temperature.

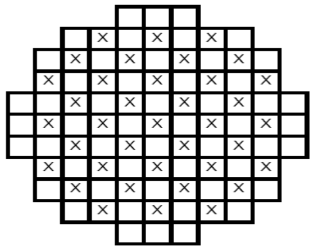

Fig.4 IRIS core configuration and a typical control rod pattern.

(a)

N/A	N/A	N/A			
0.4 IFBA	0.4 IFBA	0.4 IFBA	N/A		
0.4 IFBA	0.5 IFBA	0.4 IFBA	0.4 IFBA	N/A	
0.5 IFBA	0.5 IFBA	0.5 IFBA	0.4 IFBA	N/A	
0.6 IFBA	0.6 IFBA	0.56 IFBA	0.5 IFBA	0.4 IFBA	N/A
0.933 IFBA	0.933 IFBA	0.6 IFBA	0.5 IFBA	0.4 IFBA	N/A

(b)

N/A	N/A	N/A			
0.561 IFBA	0.561 IFBA	0.561 IFBA	N/A		
0.561 IFBA	0.561 IFBA	0.561 IFBA	0.561 IFBA	N/A	
0.561 IFBA	0.561 IFBA	0.561 IFBA	0.561 IFBA	N/A	
0.561 IFBA	0.561 IFBA	0.561 IFBA	0.561 IFBA	0.561 IFBA	N/A
0.561 IFBA	0.561 IFBA	0.561 IFBA	0.561 IFBA	0.561 IFBA	N/A

Fig.5 The 1/4 of IFBA configuration for (a) ThO_2-UO_2 and (b) ThO_2-PuO_2.

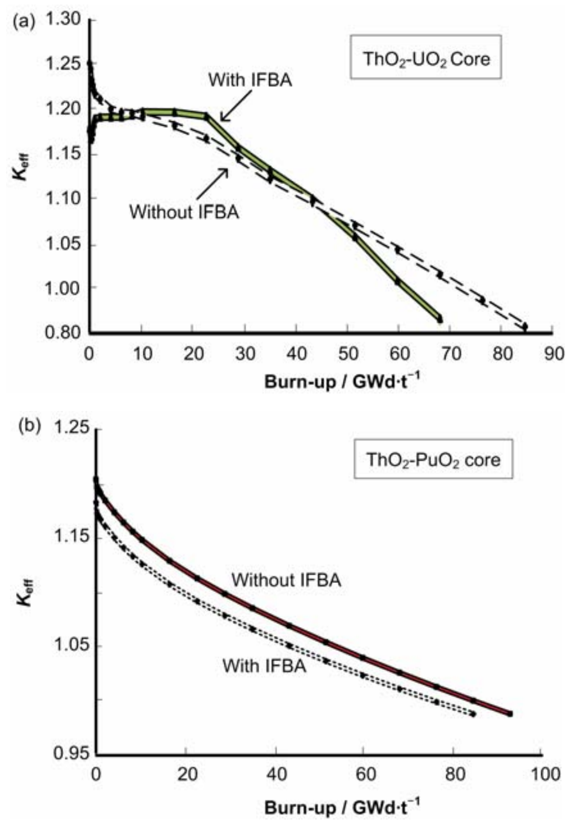

Fig.6 $K_{\rm eff}$ *vs.* burn-up for ThO_2-UO_2 (a) and ThO_2-PuO_2 cores (b).

4 Conclusion

Neutron leakage decreases in the IRIS core, due to its larger lattice pitch of fuel, and increased moderator-to-fuel ratio. Neutron absorption in the moderator increases and causes a decrease in the thermal utilization factor. The depleted plutonium is slower than uranium because the fertile ^{238}U in natural uranium captures neutrons to produce ^{239}Pu, while the ^{235}U sustains the chain reaction to produce more neutrons. As the ^{239}Pu concentration increases in the reactor, it also undergoes fission. The production of other plutonium isotopes occurs at a slower rate than that of ^{239}Pu. Thus, uranium that has been in the reactor for a short period of time has a significant amount of ^{239}Pu relative to heavier Pu isotopes. Using IFBA as burnable absorber, K_{eff} increases at the beginning because of ^{10}B reactions with the neutrons, then the K_{eff} decreases with increasing burn-up and the curves meet at around 30 GWd/t and higher values.

References

1 Carelli M D. Nucl News, 2003, **46:** 32–42.

2 Carelli M D, Petrovic B. Nuc Eng Inter, 2006, **51:** 12–17.

3 Carelli M D, Conway L E ,Fiorini G L, *et al.* IAEA, 2001, IAEA-SR-218/35: 5.

4 Sümer Ş, Veysel Ö, Hüseyin Y. Ann Nucl Energy, 2001, **3:** 203–223.

5 Boczar P G, Dyck G R, Chan P S W, *et al.* IEAE-TECDOC-1319, Recent advances in thorium fuel cycles for CANDU reactors, thorium fuel utilization:options and trends. In: Proceedings of three IEAE meetings held in Vienna 2002, 104¨C20.

6 Radkowsky A, Segev M, Galperin A. Nucl Sci Eng, 1986, **94:** 80–86.

7 Mark J C. Sci Glob Secur, 1993, **4:** 111–128.

8 Thomas L E, Einziger R E, Buchanan, H C. J Nucl Mater, 1993, **20:** 310–319.

9 Fausto F, Petrovic B. Nuclear Engineering and Design, 2008, **238:** 3240–3252.

10 Carelli M D. Eng Design, 2004, **230:** 151–167.

11 Fausto F, Petrovic B. Ann Nucl Energy, 2008, **35:** 1587–1597.

12 Duderstadt, James J, Hamilton L J. Nuclear reactor analysis, New York: John Wiley & Sons, Inc, 1976, 170–175.

13 Marleau G., Heber A T, Roy R. A user guid for dragon version4, Montreal, polytechnique de Montréal Technical, 2009, 167–195.

14 Fowler T B, Vondy D R, Cunningham G W. Nuclear reactor core analysis code, citation, Tennessee, oak ridge national lab, 1999, 104–140.